DC STATES OF PLASMA DIODES

National Aeronautics and Space Administration

Grant NsG-29963
Project 0833

Project Leader: H. Derfler
Staff: P. Burger

Quarterly Status Report QSR No. 12

January 1 - April 1, 1965

Electron Devices Laboratory
Stanford Electronics Laboratories

Stanford University
Stanford, California

[redacted]

The purpose of this project is the study of stationary potential distributions between parallel plane electron and ion emitting surfaces.

I. INTRODUCTION

The subject of "coverage instabilities" in Caesium plasma diodes has been introduced in QRR No. 10 together with the basic equations which are believed to describe this phenomenon. In QRR No. 11 we have calculated the electron ion and atom emission rates from a tungsten surface in a Caesium atmosphere. Although the theory of Levine and Gyftopoulos[1], used in this process, is subject to some criticism, it is believed that it does give at least qualitatively the right answer. Therefore it should be adequate to describe the basic processes involved in the "coverage instabilities".

II. CALCULATION OF THE DC CHARACTERISTICS

In this report we are calculating the DC characteristic of a Caesium plasma diode to find out if a negative slope is obtained under certain critical conditions. This calculation follows closely some earlier work done in this laboratory[2,3] which should be consulted along with the theory outlined below.

In Fig. 1 we show a preconceived potential distribution together with the corresponding ion and electron orbits in their v,x phase space. We aim at making this potential distribution self consistent with the space charge equation

$$\epsilon_o \frac{dE}{dx} = \rho_p + \rho_e = e \int f_p(x,v)dv - e \int f_e(x,v)dv \ . \qquad (1)$$

Provided the potentials of collector and emitter are such that $\phi_C < \phi_E < \phi_M$, the ion and electron distribution functions obtained by the method described in Ref. 2 are given by:

$$f_p(x,v) = F_p\left[m_p \frac{v^2}{2} + \phi - \phi_E\right] \cdot H\left[v + \mathrm{sgn}(x_M - x)\left(\frac{2e}{m}\right)^{1/2}\sqrt{\phi_M - \phi}\,\right] \qquad (2)$$

$$f_e(x,v) = F_e\left[m \frac{v^2}{2} - \phi + \phi_E\right] \cdot H\left[v + \left(\frac{2e}{m}\right)^{1/2}\sqrt{\phi - \phi_C}\right] \cdot H\left[v^2 - \frac{2e}{m}(\phi - \phi_E)\right] + \qquad (3)$$

$$G_e\left[m \frac{v^2}{2} - \phi + \phi_E\right] \cdot H\left[-v^2 + \frac{2e}{m}(\phi - \phi_E)\right]$$

where F_p and F_e are the velocity distribution functions given at the emitter:

$$F_p = \gamma_p \frac{m_p}{kT} e^{-m_p v^2/2kT}, \quad F_e = \gamma_e \frac{m}{kT} e^{-mv^2/2kT} \tag{4}$$

with particle emission rates γ_p and γ_e respectively.

G_e is the velocity distribution function of the electrons within the trap $x_E < x < x_T$, symmetric in velocity but otherwise arbitrary. And finally we note that

$$H(x) = \frac{1}{2}(1 + \operatorname{sgn} x) \tag{5}$$

is the unit step function.

A sample of the electron distribution function $f_e(x,v)$ for $x_E < x < x_T$ is shown in Fig. 2. The maximum speed of the returning electrons is given by $v_c = -(2e/m)^{1/2}\sqrt{\phi-\phi_c}$ and the trapped electrons are contained between $\pm v_T$, $v_T = (2e/m)^{1/2}\sqrt{\phi-\phi_E}$. It is suggested by the Penrose criterion[4] that such a doubly-humped velocity distribution is unstable. Since this criterion was derived for uniform plasmas only and exceptions are known to exist in nonuniform plasmas[5], we are not sure that double stream instabilities will arise in the system under consideration. The "coverage instability" is due to an entirely different feedback mechanism and should occur even if the electron trap is smoothly filled with electrons such that double stream instabilities can definitely be excluded.

Proceeding with our analysis of the DC state we find it convenient to select the origin of the ϕ, x plot such that $\phi_E = 0$, $x_E = 0$ and measure potentials in units of kT/e, $\eta = e\phi/kT$. With this provision the space charge densities, obtained by performing the integrations indicated in Eq. (1), are as follows:

$$\rho_p = e\gamma_p \left(\frac{\pi m_p}{2kT}\right)^{1/2} e^{-\tau_E} Q(\mathrm{sgn}(x)\sqrt{\eta_M - \eta}) \tag{6}$$

$$\rho_e = -e\gamma_e \left(\frac{\pi m}{2kT}\right)^{1/2} \left\{ e^{\eta_c} Q(-\sqrt{\eta-\eta_c}) - H(\eta)\,[Q(-\sqrt{\eta}) - Q(\sqrt{\eta})] \right\}$$

$$-e\left(\frac{2kT}{m}\right)^{1/2} \int_{-\sqrt{\eta}}^{+\sqrt{\eta}} G_e[kT(t^2-\eta)]dt \tag{7}$$

Here

$$Q(x) = e^{x^2}\,\mathrm{erfc}(x) \equiv \frac{-i}{\pi} Z(ix) \tag{8}$$

is the function introduced in Ref. 2, which is related to the functions $F^{\pm}$ used in Ref. 3 by

$$F^{+}(x) = Q(-\sqrt{x}), \quad F^{-}(x) = Q(+\sqrt{x}) \tag{9}$$

We note that, if the potential well $x_E < x < x_T$ is to be filled with electrons such that $f_e(x,v)$ is a smooth function of velocity and distance as shown in Fig. 2 (dashed line), we must have necessarily $G_e = F_e$, in which case the last three terms in Eq. (7) cancel:

$$\rho_e = -e\gamma_e \left(\frac{\pi m}{2kT}\right)^{1/2} e^{\eta_c} Q(-\sqrt{\eta-\eta_c}); \qquad G_e = F_e \tag{10}$$

we note that for $\eta - \eta_c$ large, we have $\exp(\eta_c)\ Q(-\sqrt{\eta-\eta_c}) \to 2\exp(\eta)$ so that

$$\rho_e \to -e\gamma_e \left(\frac{2\pi m}{kT}\right)^{1/2} e^{\eta}, \qquad G_e = F_e, \qquad \eta-\eta_c > 1.5 \tag{11}$$

which is also the result of a pressure-type analysis. We see that, at the position of the potential maximum $\eta = \eta_M$, the density of the electrons is greatly increased over that of the emitter, due to the presence of the trapped electrons.

Obviously the results of the DC analysis, the voltage current characteristics, will depend largely on the amount of electron trapping allowed, which is arbitrary. In fact the amount of trapping can be determined only by a large signal RF analysis.

Since, within the framework of a DC analysis, it is a matter of personnal taste to assume the trap either empty or completely filled with electrons, we prefer the latter as being closer to statistical equilibrium. With this provision, collecting Eqs. (1), (6), (10), the space charge equation becomes:

$$-2\frac{d^2\eta}{d\xi^2} = e^{-\eta_M}\,\mathcal{C}\left(\mathrm{sgn}\,(\xi)\sqrt{\eta_M-\eta}\right) - \frac{1}{\alpha}\,e^{\eta_c}\,\mathcal{C}\left(-\sqrt{\eta-\eta_c}\right) \tag{12}$$

where

$$\eta_c < 0 < \eta_M,\ \eta_c < \eta < \eta_M$$

and

$$\alpha = \frac{\nu_p}{\nu_e}\left(\frac{m_p}{m}\right)^{1/2} \tag{13}$$

The distance $\xi = x/\lambda$ is measured in Debye lengths, defined with the equilibrium ion density at the emitter obtained for $\eta_c = +\infty$:

$$\lambda_p^2 = \frac{\epsilon_o kT}{e^2 n_p} = \frac{\epsilon_o}{e\nu_p}\left(\frac{e}{2\pi m_p}\right)^{1/2}\left(\frac{kT}{e}\right)^{3/2} \tag{14}$$

Numerically we have with $j_p = e\nu_p$:

$$\lambda_p = C\left(\frac{m}{m_p}\right)^{1/4} T^{3/4}\, j_p^{-1/2} = D\left(\frac{m}{m_p}\right)^{1/4} T^{3/4}\, \nu_p^{-1/2} \tag{15}$$

$$C = 1.0885 \times 10^{-6}\, A^{1/2}\, (^oK)^{-3/4}\ ,$$

$$D = 2.7196 \times 10^{3}\, \mathrm{sec}^{-1/2}\, (^oK)^{-3/4}$$

III. THE COMPUTER PROGRAM

Although Eq. (12) can be integrated once, it was found more convenient to program this differential equation for numerical computation, using the second order difference operator:

$$\frac{d^2\eta}{d\xi^2} = \frac{\eta(\xi+h) - 2\eta(\xi) + \eta(\xi-h)}{h^2} \tag{16}$$

The essential steps in computing the DC characteristics are as follows:

i) Input data are

$$T\ ^{\circ}K,\ T_a\ ^{\circ}K,\ d = x_C - x_E\ \text{cm},\ W_e = 1.81\ \text{volt},\ (m_p/m)^{1/2} = 492.2$$

ii) From which the arrival rate of the neutrals is calculated

$$\log \mu_a = 27.02036 - 3765/T_a \quad \text{(Ref. 1, p. 236)} .$$

iii) Pick a value for the degree of coverage θ

iv) and compute γ_a, γ_p, γ_e, W_E as shown in QRR No. 11, as well as α Eq. (13), λ_p Eq. (15)

v) Calculate η_M . In the DC case we have $d\theta/dt = 0$ hence $\mu_a + \mu_p = \gamma_a + \gamma_p$ and so:

$$\eta_M = \ell n \frac{j_{ps}}{j_p} = \ell n \frac{\gamma_p}{\gamma_p - \mu_p} = \ell n \frac{\gamma_p}{\mu_a - \gamma_a} > 0 . \tag{17}$$

vi) Pick a value for the collector potential $\eta_c < 0$.

vii) Integrate the space charge Eq. (12) from $\eta = \eta_M$, $\xi = 0$ through negative values of ξ until $\eta = 0$. The corresponding distance is $\xi_- < 0$. Thus we find

$$\xi_+ \equiv \frac{x_C - x_M}{\lambda_p} = \frac{d}{\lambda_p} + \xi_- > 0 \tag{18}$$

viii) Integrate the space charge Eq. (12) from $\eta = \eta_M$, $\xi = 0$ through positive values of ξ until $\xi = \xi_+$. At that point η should be equal to η_c, if not return to Step vi, pick another value for η_c and repeat until $\eta = \eta_c$ is true.

ix) A point of the characteristics is thus found. Corrected for contact potential it is:

$$j = e\gamma_p\, e^{-\eta_M} + e\gamma_e\, e^{\eta_c} \tag{19}$$

$$\eta_{APPL} = \eta_c - \frac{e}{kT}(W_E - W_C) \tag{20}$$

x) To obtain another point of the DC characteristic return to iii, pick another θ and repeat Steps iv through ix.

IV. THE COEXISTENCE OF SURFACE PHASES AND DIFFUSION

We note that the range of θ in this computation is limited by two conditions. First we have

$$\gamma_a + \gamma_p = \mu_a + \gamma_p \geq \mu_a \tag{21}$$

If $\gamma_a + \gamma_p = \mu_a$, no ions are reflected $\mu_p = 0$, so $\eta_M = 0$, and the maximum temperature-limited current $j = e\mu_p$ is drawn across the diode. The second condition arises from the fact that the ion current drawn across the diode must be positive thus:

$$j_p = e(\gamma_p - \mu_p) = e(\mu_a - \gamma_a) \geq 0 \tag{22}$$

The case $\mu_a = \gamma_a$ corresponds to complete space charge limitation and arises only for large positive potentials η_c which are not of interest here.

The consequences of these conditions Eq. (21) and (22) are best discussed by means of Fig. 3. In this drawing we exaggerate some of the features of Fig. 2 of QRR No. 10, on ion and neutral atom emission rates obtained from a Tungsten emitter of 1800 °K within a Caesium atomsphere. For several neutral atom arrival rates $\mu_a = \mu_{a\nu}$ we show the range of concentration $\sigma = \sigma_f \theta$ allowed for the adsorbate due to Eq. (21) and (22). According to these conditions, intersections of the lines $\mu_a = \text{const}$ with the S-shaped curve $\gamma = \gamma_a + \gamma_p$ correspond to temperature limitation and the intersections with γ_a to full space charge limitation of the ion diode. We note that the sequence of states shown in Fig. 3 can also be obtained by keeping μ_a at a fixed level ($T_a = \text{const}$) and changing the temperature T of the emitter. In this case the S-shaped curve in Fig. 3 shifts up or down relative to the one selected level of μ_a, depending on whether the temperature of the emitter is rised or lowered. Taylor and Langmuir's experiment on the evaporation of atoms, ions and electrons from Caesium films was done in this fashion. In the range $\mu_{a2} > \mu_a > \mu_{a4}$ three surface phases coexist and thus the density $\sigma = \sigma_f \theta$ of the Caesium film varies along the surface (y,z directions). Diffusion must then be taken into account. With this addition our rate equation (4) of QRR No. 10 reads:

$$\frac{d\sigma}{dt} = \mu_a + \mu_p - \gamma_a - \gamma_p + D\left(\frac{\partial^2\sigma}{\partial y^2} + \frac{\partial^2\sigma}{\partial z^2}\right) \tag{23}$$

where D is the coefficient of two-dimensional diffusion. Taylor and Langmuir's experiment was done under temperature-limited conditions thus, $\mu_p = 0$ independent of σ. A small signal analysis of Eq. (23):

$$\gamma_s + \gamma_p = \gamma = \gamma_\delta + \left(\frac{\partial\gamma}{\partial\sigma}\right)_\delta (\sigma-\sigma_\delta) + \ldots; \; \sigma \alpha \exp(-st \pm i\vec{k}\cdot\vec{y}) \tag{24}$$

then yields the characteristic equation

$$s = \left(\frac{\partial\gamma}{\partial\sigma}\right)_\delta + D(\vec{k})^2 \tag{25}$$

saying that the phase θ_δ, $(\partial\gamma/\partial\sigma)_\delta < 0$ is unstable as long as its dimensions exceed

$$|\vec{y}| = \frac{2\pi}{|\vec{k}|} = D^{1/2}\left[-\left(\frac{\partial\gamma}{\partial\sigma}\right)_\delta^{-1/2}\right] \tag{26}$$

This has already been shown by Langmuir.[7] In fact he blames this instability for "spontaneous transitions" he observed in the saturated ion current from a filament the temperature of which was varied.[6] To our knowledge the time scale of this transition has never been reported, but it must be slow if the effect is due to diffusion.

V. THE FEEDBACK OF IONS FROM THE POTENTIAL MAXIMUM

We shall now investigate the feedback of ions from the potential maximum in front of the emitter to find out whether it is a more effective means to redistribute the adsorbate between the surface phases.

As long as the diode is not temperature-limited we have $\mu_p \neq 0$, depending on the height of the potential maximum in front of the emitter. This feedback may lead to instabilities the time scale of which would be of the order of the transit time of an ion on its way against the decelerating field of the potential maximum. As a first check of this idea we have calculated the DC characteristics of a diode, neglecting the effect of the electrons. Taking $\gamma_e = 0$, the iterative step number vi in the computer program can be ignored. In fact the tables of Kleynen[8] for the thermionic diode could be used to obtain the voltage current characteristics. For numcerical purposes data were selected such as to correspond roughly to the conditions under which Dr. Breitwieser[9] observed his anomalous open circuit voltages.

Electron Temperature $T = 1800\ ^{o}K$

Caesium Temperature $T_a = 464.4\ ^{o}K$

Caesium Arrival Rate $\mu_a = 8.265 \times 10^{18}\ cm^{-2}\ sec^{-1}$

Emitter Collector Distance $d = 4 \times 10^{-3}\ cm$

Critical Densities θ	Corresponding Ion Emission $\nu_p\ cm^{-2}sec^{-1}$	$e\nu_p\ amp \cdot cm^{-2}$
$\theta_\beta = 0.03025$	7.731×10^{18}	1.239
$\theta = 0.05425$	6.734×10^{18}	1.079
$\theta_\alpha = 0.07975$	4.595×10^{18}	0.736
$\theta_\alpha' = 0.10640$	2.790×10^{18}	0.447

The voltage current characteristics obtained with these data are shown in Fig. 4. We first notice the three distinct saturation levels associated with the three surface phases θ_β, θ_δ, θ_α respectively. These saturation levels apparently break away at sharp angles from the almost ideal Child-Langmuir space charge characteristics. We did expect a negative slope of the characteristics near the point "S" in Fig. 4. Since we could not resolve this region due to numerical limitations of the computer we made an analytic series development near that Saturation Point S, the details of which are omitted here. For our example we found

$$\frac{V-V_s}{V_s} = -5.65 \times 10^{-3}\left(\frac{j-j_s}{j_s}\right)^{1/2} + 0.66\left(\frac{j-j_s}{j_s}\right) + \ldots \qquad (27)$$

from which we deduce the point of zero incremental resistance:

$$\frac{dV}{dj} = 0 \quad \text{at:} \quad \frac{V_s-V^*}{V_s} = 18.4 \times 10^{-6}\ , \ \frac{j^*-j_s}{j_s} = 12.2 \times 10^{-6} \qquad (28)$$

It was thus found that the region of negative slope is very small. This is shown in Fig. 5, which is a qualitative interpretation of the computed results shown in Fig. 4. At this stage we do not know whether this short interval of negative

resistance $V^* < V < V_s$ will lead to instabilities other than those due to surface diffusion as described by Langmuir. We do know, however, that at much shorter emitter collector distances "d" this region of negative resistance becomes substantially larger. It is expected that the addition of electrons $\gamma_e \neq 0$ has about the same effect as decreasing the distance d. Computations of the DC characteristics, allowing for trapped electrons, are now in progress to check this point.

REFERENCES

1. J.D. Levine and E.P. Gyftopoulos, Surface Physics, 1, 1964, pp. 171-193 and pp. 225 - 241.

2. H. Derfler, Phys. of Fluids, 7, 1964, pp. 1625-1637.

3. P. Burger, Technical Report No. 0254-1, April 1964, Stanford Electronics Laboratories, Stanford University, Stanford, California.

4. O. Penrose, Phys. Fluids, 3, (1960), p. 258.

5. F.R. Holmstrom, Technical Report No. 0832-2, Stanford Electronics Laboratories, Stanford University, California.

6. J.B. Taylor and I. Langmuir, Phys. Rev., 44, (1933), p. 440.

7. I. Langmuir, J. Chem. Phys., 1, (1933), p. 202.

8. P.H. Kleynen, Philips Res. Rep., 1, (1946), p. 97.

9. Dr. R. Breitwieser, NASA, Lewis Research Center, Cleveland, Ohio, private communication.

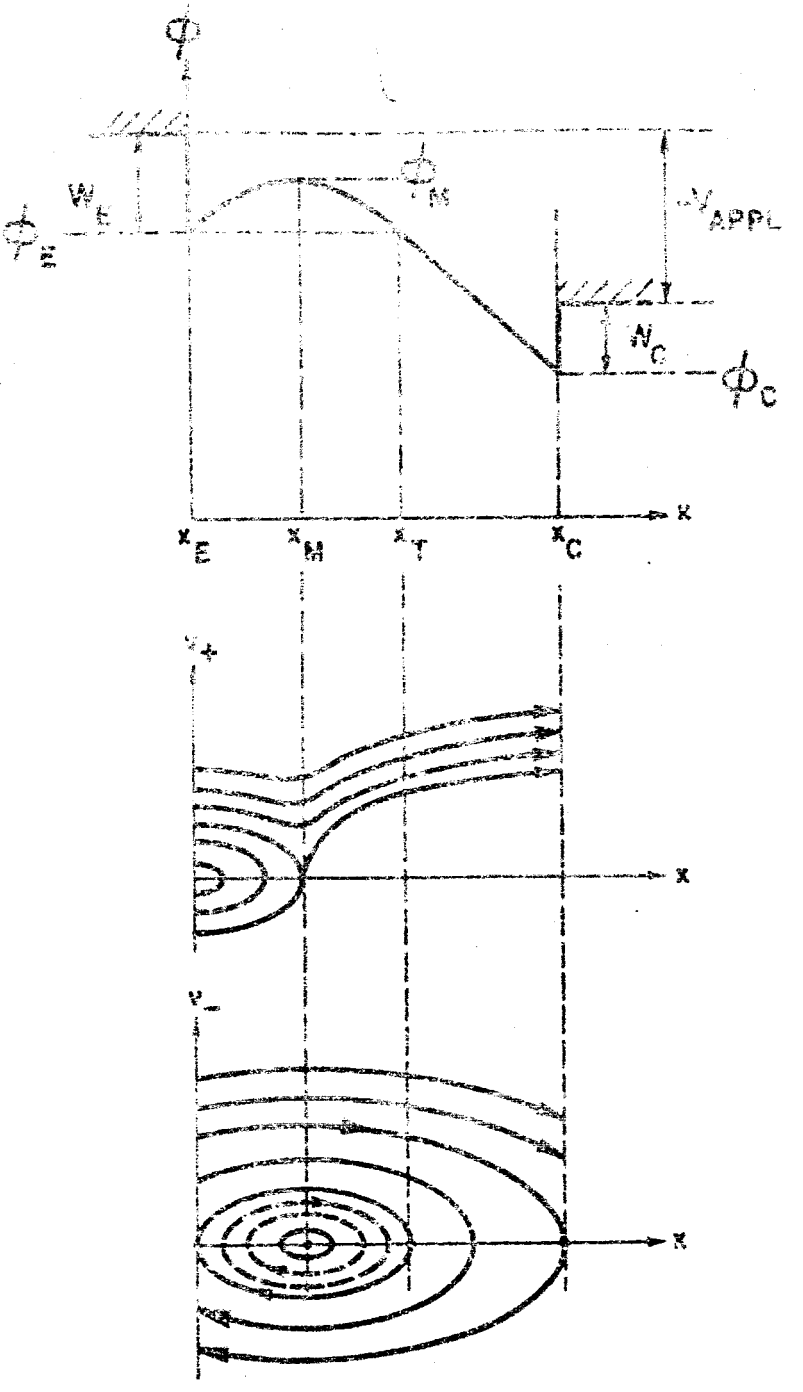

Fig. 1--a) Potential Diagram of Ion Diode
b) Corresponding Ion Orbits
c) Corresponding Electron Orbits
--- Trapped Electrons

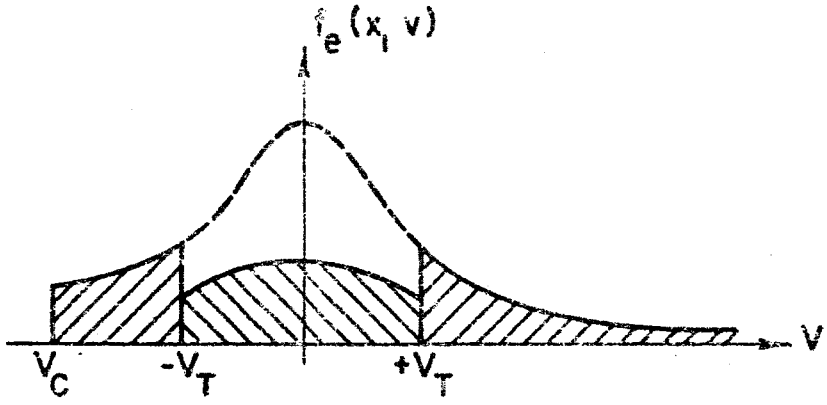

Fig. 2--Electron Distribution Function at positions $x_c < x < x_T$.

\\\\ Trapped Electrons.

--- Trap completely filled.

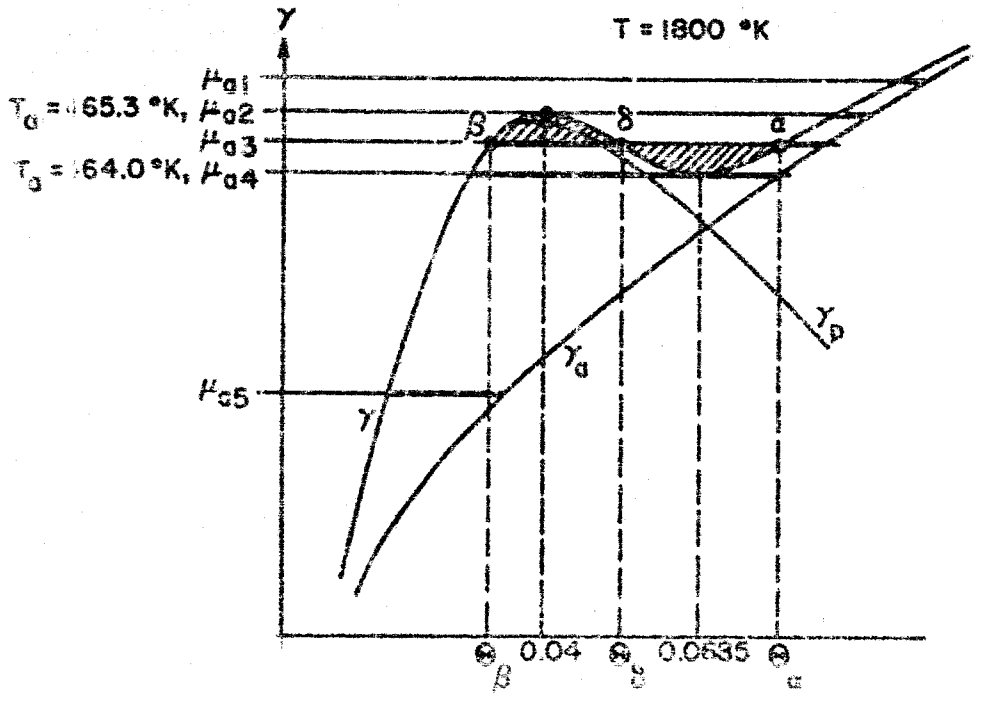

Fig. 3--Evaporation Rates of Atoms γ_a, Ions γ_p and Particles $\gamma_a + \gamma_p = \gamma$ as a function of adsorbate density Θ, for a fixed Emitter Temperature (schematic).

——— Admissible Range of density Θ for a fixed arrival rate of neutral Caesium Atoms.

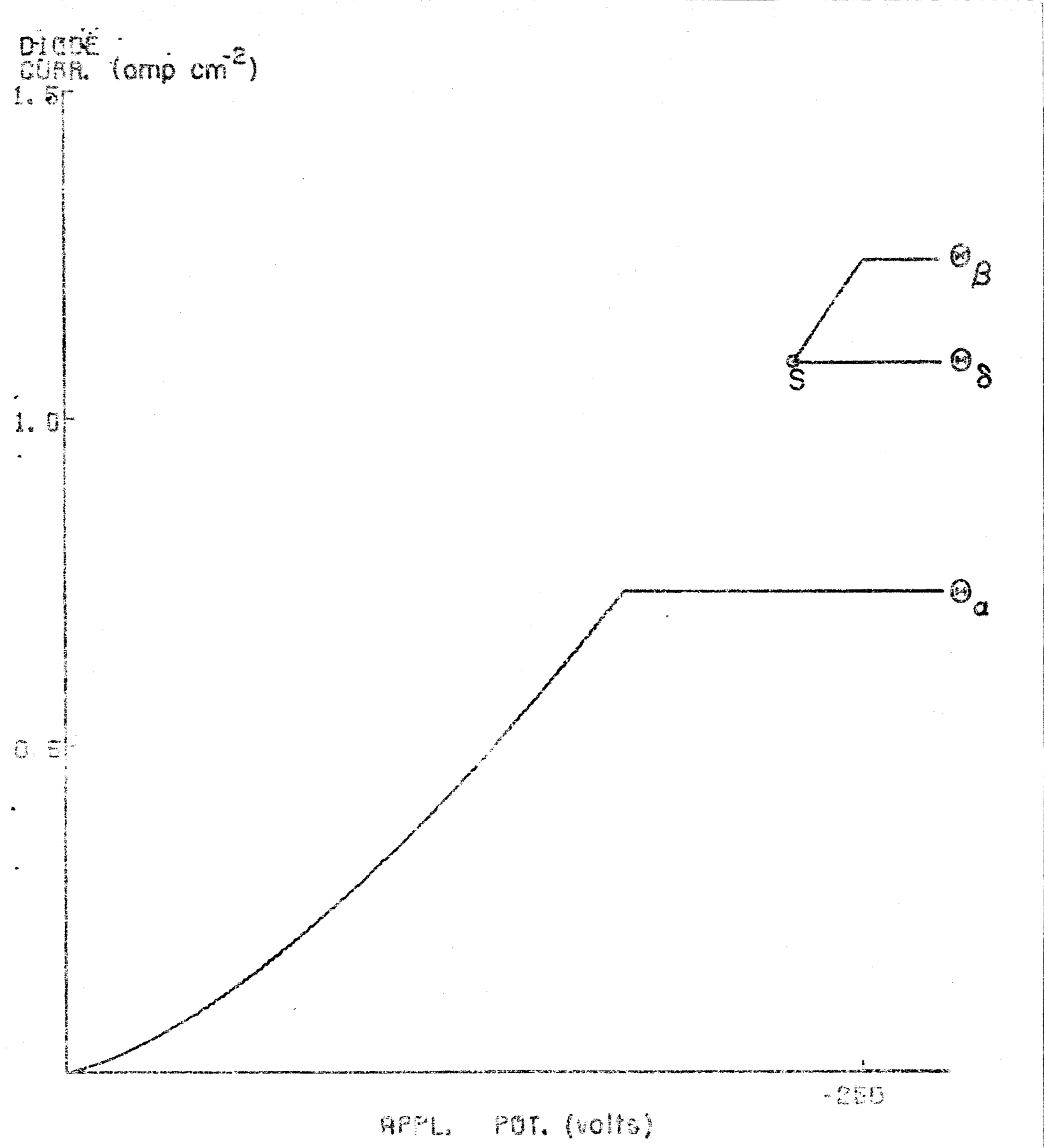

Fig. 4--Computed Ion Diode Characteristics neglecting the effect of trapped electrons.
"S"- Saturation Point due to unstable δ-phase

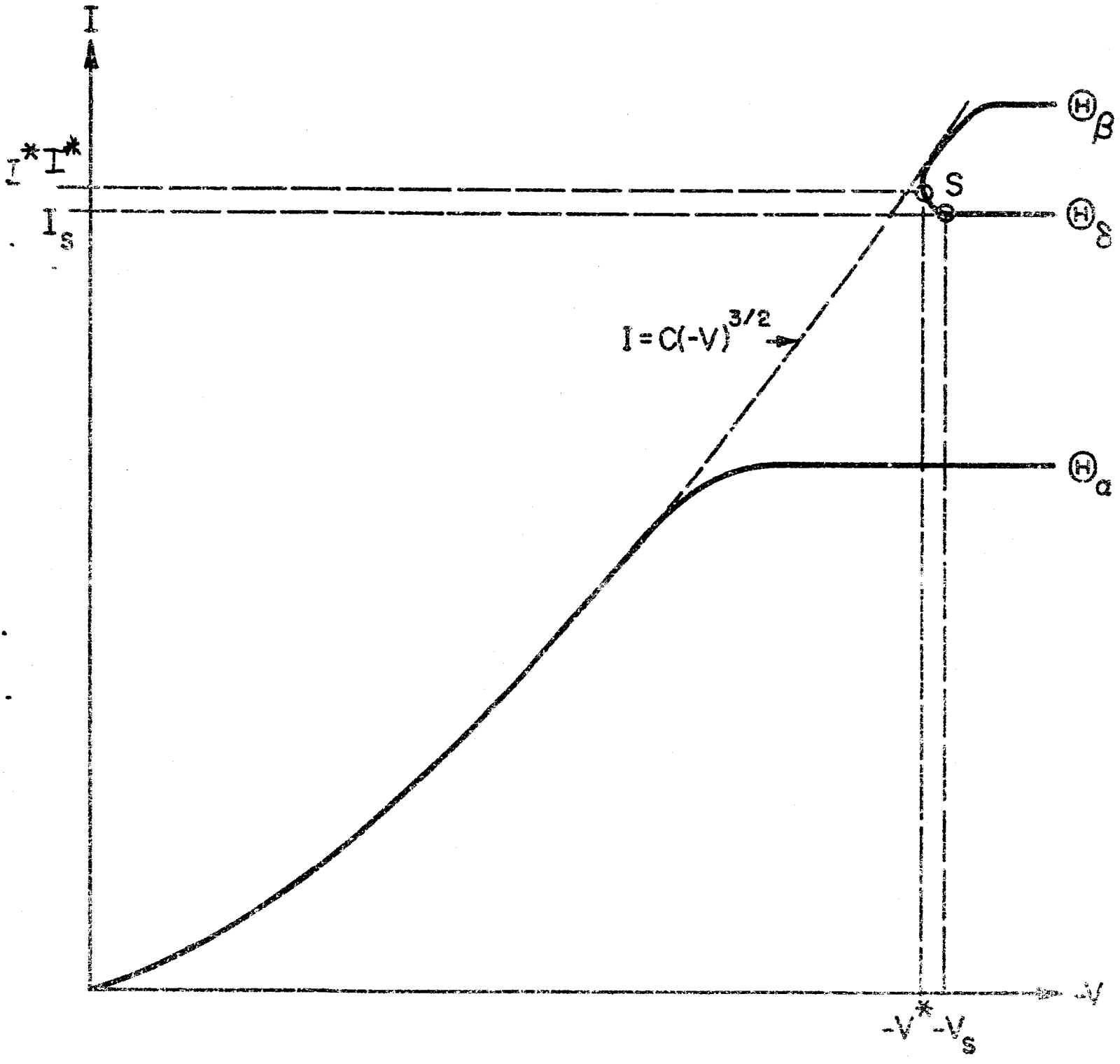

Fig. 5--Ion Diode Characteristics, schematic.
"S" - Saturation Point due to the unstable δ-phase.
$-V^* < -V < -V_S$ unstable region.

PROJECT 0254: PLASMA THERMIONIC DIODES

National Aeronautics and Space Administration Grant NsG 299-63
Project Leader: O. Buneman
Staff: P. Burger, Gregory Heath

The purpose of this project is to study the randomization of electron energies in thermionic diodes by computer methods.

The analysis of the low pressure thermionic converter has been completed. Results for the converter can be found in earlier QRRs and in an article that will be published shortly in the Journal of Applied Physics.

We have begun expanding the present computer program (which was able to simulate collisionless plasma diodes) in two directions. First, the emission properties of a hot tungsten plate partially covered with cesium are simulated. Secondly, electron-neutral and ion-neutral collisions are simulated by random processes.

1. Time-Variable Surface Emission

In our earlier work with the low pressure thermionic converter the operation of the emitter was idealized by assuming constant saturation currents for electrons (J_{se}) and ions (J_{si}). Since the emitter of the thermionic converter is a hot tungsten plate partially covered with cesium, the emission properties of the plate are determined by the fractional cesium coverage of the emitter. The equations for the emission rates of electrons and ions are given in QRR No. 10, under project 0833.

The functional dependence of the emitted currents on cesium coverage will not be reproduced here; we will write $J_{se} = J_{se}(\theta)$, $J_{si} = J_{si}(\theta)$, showing that functional relationships exist between the currents and θ, the cesium coverage. The important equation for our purpose is the change of coverage in time, which is given by:

$$\frac{\partial \theta}{\partial t} = C_f(\mu_a + \mu_i - \gamma_a - \gamma_i) \qquad (1)$$

where C_f is a known constant; μ_a and μ_i are the arrival rates of atoms and ions respectively; and γ_a, γ_i are the evaporation rates of atoms and ions respectively. The arrival rate of atoms is assumed to be a constant, which depends only on the pressure of the neutral cesium gas. The evaporation rates

of atoms and ions are determined from the existing cesium coverage. (Note that $\gamma_i = J_{si}(\epsilon')/|e|$ where $|e|$ is the electronic charge.) The arrival rate of ions, determined by the computer simulation procedure, is the number of ion sheets that reach the emitter surface during one time step, divided by the length of the time step. If we call the successive time steps in the computer simulation procedure $t_1, t_2, \ldots, t_n, \ldots$ and the time step $\Delta t = t_{n+1} - t_n = t_n - t_{n-1}$, etc., then in difference equation form:

$$\frac{\theta(t_{n+1}) - \theta(t_{n-1})}{2\Delta t} = C_f(\mu_a + \frac{M_i(t_n)}{\Delta t} - \gamma_a - \frac{J_{si}(t_n)}{|e|} \qquad (2)$$

or

$$\theta(t_{n+1}) = \theta(t_{n-1}) + 2C_f\,\Delta t(\mu_a - \gamma_a) + 2C_f[\,M_i(t_n) - N_i(t_n)] \qquad (3)$$

where $M_i(t_n)$ is the number of ion sheets that arrive at the emitter at time t_n, and $N_i(t_n)$ is the number of ion sheets that are injected at time t_n calculated from the value of the cesium coverage at this time. The computations start with initial conditions $\theta(0) = \theta(\Delta t) = 0$, i.e. the coverage is zero initially. Since the diode is empty at the beginning of the calculations, $M_i = 0$; similarly, because of zero cesium coverage, $\gamma_a = N_i = 0$. From Eq. (3), then, $\theta(2\Delta t) = 2C_f\mu_a\Delta t$. At later times the calculations of the trajectories of ions and electrons are made using a step-by-step procedure similar to our earlier computer simulation calculations. The numbers of injected ion and electron sheets are determined at every time step from the given cesium coverage. The computer programs that will execute all these functions are being written and checked at the present.

2. Electron-Neutral Elastic Collisions

Our plan of introducing electron-neutral elastic collisions into our model is the following. An electron sheet is injected into the diode at time t_i with velocity $u_{\parallel}(t_i)$ in the direction of motion of the sheet and with velocity $u_{\perp}(t_i)$ perpendicular to the direction of motion of the sheet. The

perpendicular velocity is ignored as long as the sheet moves without making a collision. At time t_c the sheet suffers a collision. At this time the parallel velocity of the sheet is $u_{\parallel}(t_c)$, which is not the same as its initial velocity $u_{\parallel}(t_i)$, since the sheet was accelerated by electric fields. The perpendicular velocity component has not changed. The energy of the sheet is proportional to the sum of the squared velocities: $u^2(t_c) + u_{\perp}^2(t_i)$, which is $u_T^2(t_c)$, the total velocity squared of the sheet at the time of collision. The total velocity of a sheet, $u_T(t_c) = \sqrt{u_{\parallel}^2(t_c) + u_{\perp}^2(t_i)}$, remains constant during a collision. The collision is assumed to be spherically symmetric; therefore we can express the parallel velocity of the sheet after collision as $u_{\parallel}^*(t_c) = R \cdot u_T(t_c)$, where R is a random variable uniformly distributed in the interval $-1 \leq R \leq 1$. Thus, during computations we obtain a number from a random sequence of numbers that are distributed uniformly in this interval and determine the parallel velocity of the sheet after collision. The perpendicular velocity after the collision is $u_{\perp}(t_c) = \sqrt{u_T^2(t_c) - [u_{\parallel}^*(t_c)]^2}$. The perpendicular velocity remains a constant for the sheet until the next collision occurs.

Initial arrangements are being made to introduce the described collision concept into the computer program of the simulated plasma diode.